Hydroxyapatite whiskers provide improved mechanical properties in reinforced polymer composites

Ryan K. Roeder,[1] Michael M. Sproul,[2] Charles H. Turner[2,3]
[1]*Department of Aerospace and Mechanical Engineering, University of Notre Dame, 381 Fitzpatrick Hall, Notre Dame, IN 46556-5637*
[2]*Biomedical Engineering, Indiana University—Purdue University at Indianapolis, Indianapolis, IN 46202*
[3]*Department of Orthopedic Surgery, Indiana University Medical Center, Indianapolis, IN 46202*

Received 4 September 2002; revised 28 March 2003; accepted 2 May 2003

Abstract: Synthetic hydroxyapatite (HA) whiskers have been utilized as a new, biocompatible reinforcement for orthopedic biomaterials. High-density polyethylene (HDPE) was reinforced with either the synthesized HA whiskers or a commercially available spherical HA powder using a novel powder processing technique that facilitated uniform dispersion of the reinforcements in the matrix prior to compression molding. Composites were processed for up to 60 vol % HA whiskers and up to 50 vol % spherical HA. The mechanical properties of the new composite biomaterials were examined by uniaxial tensile tests. As expected, increased volume fraction of either reinforcement type over 0–50 vol % resulted in increased elastic modulus, a maximum in ultimate tensile stress, and decreased work to failure. Composites reinforced with HA whiskers had higher elastic modulus, ultimate tensile strength, and work to failure relative to composites reinforced with spherical HA. Thus, HA whisker-reinforced HDPE composites possessed improved mechanical properties over those reinforced with spherical HA. HA whisker-reinforced composites were anisotropic due to alignment of the whiskers in the matrix during processing. © 2003 Wiley Periodicals, Inc. J Biomed Mater Res 67A: 801–812, 2003

Key words: orthopedics; bone substitutes; hydroxyapatite; polyethylene; anisotropy

INTRODUCTION

Improved orthopedic biomaterials for bone substitutes are needed in the treatment of diseased bone (e.g., osteoporosis), injured bone (e.g., fractures), or bone defects.[1–3] Optimum synthetic biomaterials for load-bearing orthopadic implants must meet biologic, functional, and mechanical performance criteria.[1,2] At minimum, the biomaterial must be biocompatible, but may also possess the added benefit of being bioactive, bioresorbable, osteoconductive, or osteoinductive depending on the surgical procedure, implant site, and patient indications. Functional criteria include factors such as shapability, deliverability, and the cost of the biomaterial. Successful biomaterials have possessed a range of mechanical properties, but an ideal synthetic biomaterial should hypothetically match the mechanical properties of the surrounding host tissue. To date, there have been no synthetic bone substitutes possessing both the mechanical and biologic properties required to adequately test this hypothesis. For example, autografts and allografts, despite well-documented drawbacks, remain the gold standard over synthetic bone substitutes.[1–3] Further, implants with an elastic modulus that significantly exceeds that of the surrounding host tissue are thought to cause stress shielding and contribute to degradation of the host tissue.[4,5]

Cortical bone in the human femoral shaft has an elastic modulus of 17–27 and 6–13 GPa, and tensile strengths of 80–150 and 50–60 MPa, in the longitudinal (along bone axis) and transverse directions, respectively.[1,6,7] Cancellous bone has an effective elastic modulus and tensile strength in the range of 0.05–0.5 GPa and 1–20 MPa, respectively, depending on the apparent density.[1,6,7] While the effective properties of cancellous bone are significantly lower than cortical bone due to the highly porous structure (typically 70–95% porosity), the actual trabecular tissue properties are similar to cortical bone.[6–8] Thus, the metallic implants most commonly used today, as well as dense

Correspondence to: R.K. Roeder; email: rroeder@nd.edu
Contract grant sponsor: State of Indiana 21st Century Research and Technology Fund

ceramics, have mechanical properties that are typically an order of magnitude greater than bone tissue. A stiff metal device acts to "shield" the adjacent bone tissue from mechanical stresses. When bone tissue is insufficiently loaded the relative rate of bone resorption by osteoclasts exceeds the rate of new bone formation by osteoblasts, resulting in a weakened bone and bone–implant interface. Efforts to utilize porous ceramics or poly(methyl methacrylate) (PMMA) bone cement in place of stiffer materials have been limited by the low fracture toughness of these materials, as well as other functional and biologic issues. Finally, thermoplastic polymers offer many potential advantages,[1] especially for tissue engineering scaffolds,[9] but are alone too weak and compliant for load-bearing applications.[2]

To remedy the mechanical mismatch problems, such as stress shielding, associated with most currently available orthopedic biomaterials, much work has been dedicated to producing synthetic biomaterials that match the mechanical properties of human bone tissue. Composite materials offer a rational design approach but have not yet found significant clinical success.[10] Particulate-reinforced polymers have comprised a popular design approach due to considerations such as cost and ease of processing. Calcium phosphates, typically hydroxyapatite or β-tricalcium phosphate, have comprised a logical choice for the reinforcement phase based on similarities to human bone mineral. Consequently, many research groups have developed a variety of calcium phosphate-reinforced polymer composites, including hydroxyapatite (HA)- reinforced polyethylene,[11–14] polylactide,[15–18] and polyacrylics,[19–22] to name a few. Perhaps the most extensive work to date was in the development of HAPEX, an HA-reinforced high-density polyethylene (HDPE).[11–14] However, despite significant improvements, these isotropic composites, as well as the other works cited above, still remained well short of the mechanical properties of bone tissue—too compliant and weak to be used for most load-bearing orthopedic applications.

As a material, bone contains directional structural features across several hierarchical scales, ranging from nanoscale crystals and molecules to the macroscopic shape.[7] Each hierarchical scale has unique features and directionality that influence the anisotropic properties and *in vivo* processes in the living tissue. However, the foundational structural unit across all scales is a relatively simple two-phase arrangement of reinforcement and matrix. A matrix of oriented collagen molecules is reinforced with a distribution of oriented, anisometric crystals of bone mineral. Bone mineral crystals have an elongated c-axis (either plate or whisker shaped), and most closely resemble HA in chemical composition and crystal structure. Cortical bone mineral crystals in the bovine femur have been measured to have an overall preferred orientation of 8–14 MRD (multiples of a random distribution) along the longitudinal bone axis.[23–25] Mechanical anisotropy in human cortical bone is largely due to alignment of bone mineral crystals[26] and has been characterized.[27,28] However, to date, virtually no work has been dedicated to producing synthetic biomaterials that match the mechanical anisotropy present in bone tissue.

The purpose of this study was to produce a novel biomaterial that mimics one aspect of the structure of human bone tissue that has been given relatively little attention, namely, the preferred orientation of bone mineral. We hypothesized that anisotropic mechanical properties nearly matching those of human bone tissue could be achieved by reinforcing a polymer matrix with anisometric reinforcements that are aligned during processing. To this end, synthetic HA whiskers (short single-crystal fibers) have been utilized as a new, biocompatible reinforcement for orthopedic biomaterials. A variety of matrix materials for a range of potential applications are also being explored. In this work, HDPE was chosen as an exemplary matrix material by virtue of Food and Drug Administration approval[14,29] and ease of processing. We report the processing and characterization of HA whisker-reinforced HDPE.

EXPERIMENTAL METHODS

HA whisker reinforcements

HA whisker reinforcements were synthesized at low temperature (≤ 200°C) from chemical solutions containing calcium, phosphate, and a calcium chelating agent. The technique was developed elsewhere and is often termed the "chelate decomposition method."[30–34] Homogenous solutions were prepared by adding 0.10*M* DL-lactic acid [$CH_2CH(OH)COOH$, Sigma Chemical Co., St. Louis, MO], 0.03*M* phosphoric acid (H_3PO_4, Sigma Chemical Co.), and 0.05*M* calcium hydroxide [$Ca(OH)_2$, Aldrich Chemical Co., Inc., Milwaukee, WI] to distilled, deionized water at room temperature and dissolving under constant stirring for ≈2 h. The molar ratio of P to Ca in solution was 0.6, which is equivalent to that of stoichiometric HA. Solutions were filtered, measured for pH (pH ≈ 4.0), and stored under nitrogen.

HA whiskers were precipitated from the chemical solution under hydrothermal conditions. 1250 mL of the solution was placed in the Teflon liner of a stainless steel pressure reactor (Model 4600, Parr Instrument Co., Moline, IL) and purged with nitrogen. To provide uniform thermal transport, 250 mL of distilled, deionized water was placed in the gap between the liner and stainless steel vessel. Reaction

conditions were controlled by a heating assembly (Model 4910, Parr Instrument Co.) and temperature controller (Model 4840, Parr Instrument Co.). The reaction temperature was measured by a thermocouple placed inside the thermowell of the vessel. All reactions were ramped to 200°C in 2.5 h and held at 200°C for 1.0 h. The autogenous pressure reached a maximum of 14 MPa at 200°C. After the reaction, the reactor was cooled to less than 100°C within 1 h using an aluminum block and cooling fan. The precipitated whiskers were separated from the supernatant solution by vacuum filtration. The whiskers were then washed under constant flow of 1250 mL of distilled, deionized water and dried in an oven at 80°C for at least 12 h.

The crystallographic phase of the precipitated whiskers was characterized by powder X-ray diffraction (XRD) (D5000, Siemens Analytical X-Ray Instruments Inc., Cherry Hill, NJ) using Cu Kα radiation generated at 50 kV and 40 mA. Powders were examined over 20–60° two theta with a step size of 0.02° and step time of 1.0 s. The size and morphology of the precipitated whiskers was characterized using quantitative stereology. Measurements of whisker length, width, and aspect ratio were taken using an optical microscope (Optiphot-2, Nikon, Tokyo, Japan) and a digital camera (Optronics, Goleta, CA) connected to a stereology software package (Bioquant 98, R&M Biometrics, Inc., Nashville, TN). Microscopy slides were prepared by ultrasonically dispersing 0.003 g of the whiskers in 1 mL of methanol and pipetting drops of the suspension onto a glass slide placed in an oven at 80°C to quickly evaporate the methanol. All slides were analyzed at 400× magnification. A 10 × 10 square grid was digitally overlaid using the imaging software to facilitate random whisker selection. The length and width was measured and recorded for each whisker located at grid intersections. The aspect ratio of each whisker was calculated by dividing the length by the width. A total of 500 whiskers were measured in this manner.

Spherical HA reinforcements

A commercially available equiaxed (spherical) HA powder (Product 21221, Fluka Chemical Corp., Milwaukee, WI) was used as a control for comparison to the HA whisker reinforcements. The commercial HA powder was ground using a mortar and pestle to break up any agglomerates present in the as-received powder. The crystallographic phase and morphology of the commercial powder was characterized by XRD and quantitative stereology, respectively, using the same techniques described above for the HA whiskers reinforcements.

HDPE powder

HDPE polymer powder was produced from commercially available HDPE polymer beads (Product 427977, Aldrich Chemical Co.). The polymer beads were dissolved in boiling *p*-xylene (Fisher Scientific, Acros Organics, Fairlawn, NJ) under rapid stirring. The solution was allowed to reflux under a nitrogen blanket for 10 min and then cooled to room temperature while still under rapid stirring. Upon cooling to ≈83°C, polymer particles were precipitated from the solution. The HDPE precipitates were vacuum filtered and dried in an 80°C oven for 3–12 h. After drying, the precipitates were washed with ethanol (Aldrich Chemical Co.) to remove residual xylene and homogenized with a high-speed blender (Model 909, Hamilton Beach/Procter-Silex, Inc., Washington, NC). The powder was again vacuum filtered and dried in an oven at 80°C for 1–4 h. The HDPE powder was characterized by XRD and optical microscopy using techniques similar to those described above for the HA whiskers.

HA-reinforced HDPE composite processing

Reinforced polymer composites were produced using either the synthesized HA whiskers or the commercially available spherical HA powder as reinforcements. Using the desired volume of the final composite (3.4 cm^3) and the known densities of the HA and HDPE powders (3.10 and 0.96 g/cm^3, respectively), the appropriate masses of HA and HDPE powder was measured to produce composites containing 10, 20, 30, 40, 50, and 60 vol % HA reinforcements.

Powder suspensions were prepared to provide an intimate, uniform mixture of the HA and HDPE powders. For each composite produced, the HA and HDPE polymer powders were ultrasonically co-dispersed in ethanol at 14.5 vol % total solids loading using a sonic dismembrator (Model 2020, Fisher Scientific, Pittsburgh, PA) pulsed at 1.0 cycle/s under constant stirring. The HA powder was first added to the ethanol and ultrasonically dispersed for 1 min before adding the HDPE powder and ultrasonically dispersing another 5 min. Wet co-consolidation of the HA and HDPE powders was performed by vacuum filtration immediately after dispersing. The resultant particulate composite mixture was dried in an oven at 80°C for at least 12 h to remove residual ethanol.

Two thermomechanical processing steps were used to produce dense composite bars from the particulate mixture. First, each particulate composite mixture was densified by uniaxial pressing at ambient temperature using a 10-mm diameter cylindrical pellet die. Pressure was applied to 45 MPa using a hydraulic platen press (Model 3912, Carver Laboratory Equipment, Inc., Wabash, IN). The dense composite pellets were then subjected to a second thermomechanical processing step to align the HA particles and shape the composite. A channel die was specially fabricated to compression mold dense composite pellets into 2.6 × 10 × 120-mm bars using the hydraulic platen press. The composite pellets were vertically placed in pairs at the center of the mold and the mold was heated above the melting temperature of HDPE to 145°C. Upon compression molding the viscous reinforced polymer was extruded bilaterally to the open ends of the mold. The polymer solidified as the mold was allowed to cool for 10 min on the platen press (to ≈80°C). The mold was then moved to a water-cooled aluminum block until it reached room temperature.

Additional composites containing 20 vol % HA whiskers were processed and annealed near the melting point of the HDPE polymer to examine the effects of preferred molecular orientation in the polymer matrix. Composite bars processed as above were returned to the mold and heated to 130°C. The mold temperature reached 130°C in ≈90 min and was held at temperature for 20 min. The mold was then cooled in a manner consistent to that described previously.

Composite characterization

The mechanical properties of the new composite biomaterials were examined by uniaxial tensile tests. Two ASTM standard D 638-98, Type V, tensile specimens were machined from the halves of each composite bar processed such that the extrusion direction during molding corresponded to the tensile axis. Machining was performed using a template and router bit on a high-speed end mill. Thus, for each experimental group three composite bars were processed, yielding five tensile specimens ($n = 5$) and one specimen for microstructural analysis. All tensile tests were performed using a screw-driven testing machine (Q-Test, MTS Systems Corp., Eden Prairie, MN) following ASTM standard D 638-98 for reinforced polymer composites. Tensile tests were conducted under ambient conditions at a crosshead speed of 1 mm/min. A digital extensometer (Model 632.26E-20, MTS Systems Corp.) was used to directly measure strain within the specimen gage length for accurate measurement of the elastic modulus. The elastic modulus (E), ultimate tensile stress (UTS), and work to failure (w_f) were calculated from force-displacement data and are reported. The failure surface of tensile specimens corresponding to the median specimen in each group was sputter-coated with Au-Pd and examined using a scanning electron microscope (SEM) (AMRAY SEM, AMR Corp., Bedford, MA).

Analysis of variance (ANOVA) (Statview 5.01, SAS Institute Inc., Cary NC) was used to compare the reinforcement type (whisker vs equiaxed), volume fraction, and annealing treatment. Two-way ANOVA was used to examine interactions between these experimental variables. Post-hoc comparisons were performed using a Fisher's protected least significant difference test. A log transform of the data for work to failure was used to provide a normal distribution for statistical analysis.

The preferred crystallographic orientation of HA in the composites was characterized by XRD (D5000, Siemens Analytical X-Ray Instruments Inc., Cherry Hill, NJ) using Cu Kα radiation generated at 50 kV and 40 mA. Polished sections for each of the three orthogonal specimen directions (orthogonal to the length, width, and thickness of the composite bar) were examined over 20–60° two theta with a step size of 0.02° and step time of 1.0 s. For comparison, human cortical bone specimens were taken from the proximal end of a femoral midshaft provided by the Indiana Regional Blood Center and Tissue Bank. The donor was a 22-year-old female Caucasian presenting no pathology or toxicology. Thick sections (≈ 500 μm) were deproteinized by soaking 72 h in 7% NaOCl. A powdered bone mineral sample was prepared by grinding deproteinized sections using a mortar and pestel. Polished sections were prepared for each of the three orthogonal, anatomic directions (orthogonal to the length, radius, and circumference of the femoral shaft) and examined as above. All composite and human cortical bone sections were cut using a diamond wafering saw, embedded in methacrylate, and polished to a 0.05-μm Al_2O_3 final finish.

RESULTS

Starting powders

The size and morphology of the as-prepared commercial, spherical HA powder, HA whiskers, and HDPE powder are shown qualitatively by the optical micrographs in Figure 1. Note the difference in scale of Figure 1(a) relative to Figures 1(b) and 1(c). The commercial, spherical HA powder was measured to have an average diameter of 1.3 ± 0.4 μm. The HA whiskers were measured to have an average length of 18.0 ± 8.9 μm, an average width of 2.3 ± 0.8 μm, and an average aspect ratio of 7.9 ± 3.4 μm. Note that the HA whiskers were single crystals as revealed by their transparency to transmitted light. The particle size distributions of the two types of HA reinforcements are shown in Figure 2. The size of the HDPE powder was not measured quantitatively due to irregularities in particle shape and agglomeration. However, as can be seen from the representative micrograph in Figure 1, the individual particles were in general spherical and on the order of 5–50 μm.

XRD patterns revealed that the HA whiskers were phase pure, while the commercial, spherical HA powder contained small amounts of β-tricalcium phosphate (β-TCP) (Fig. 3). β-TCP is known to form with heat treatment or calcination of Ca-deficient HA above 800°C.[35] The peaks observed for the HDPE powder are indicative of a semicrystalline polymer.

Composite processing

Composite bars were processed with up to 60 vol % HA whiskers and up to 50 vol % spherical HA. Occasional cracking was observed perpendicular to the direction of flow (the length of the bar) during compression molding in the 50 vol % spherical HA composites. Otherwise, the molded composite bars for all volume fractions of either type of HA reinforcement were reliably and repeatedly processed.

The ability to process composites at such a high ceramic content was partially limited by an inability to evaluate the mechanical properties using the procedures of this study. The brittleness of the 60 vol % HA

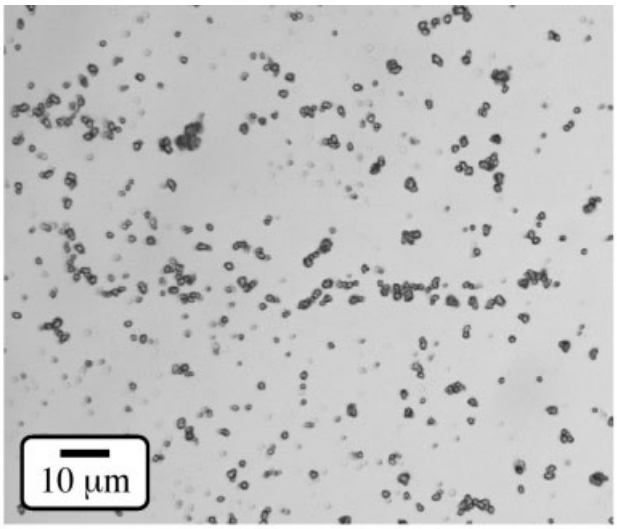

(a)

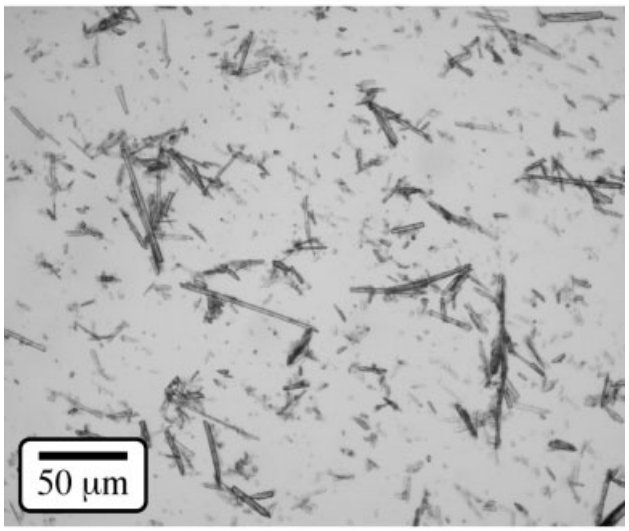

(b)

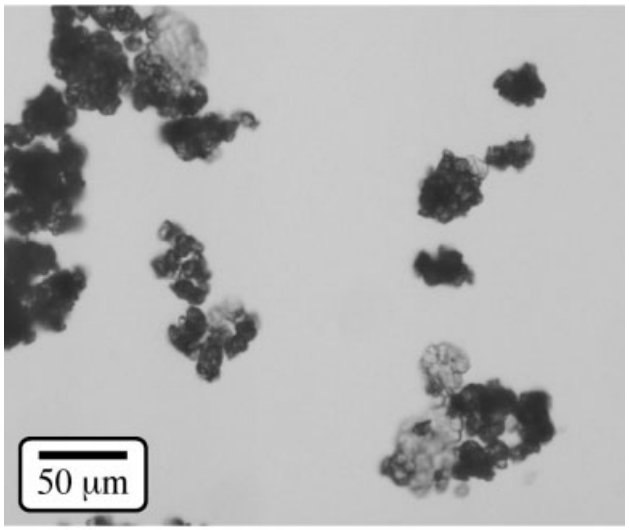

(c)

Figure 1. Transmitted light optical micrographs of the as-prepared starting powders: (a) commercial, spherical HA powder; (b) HA whiskers; (c) HDPE powder.

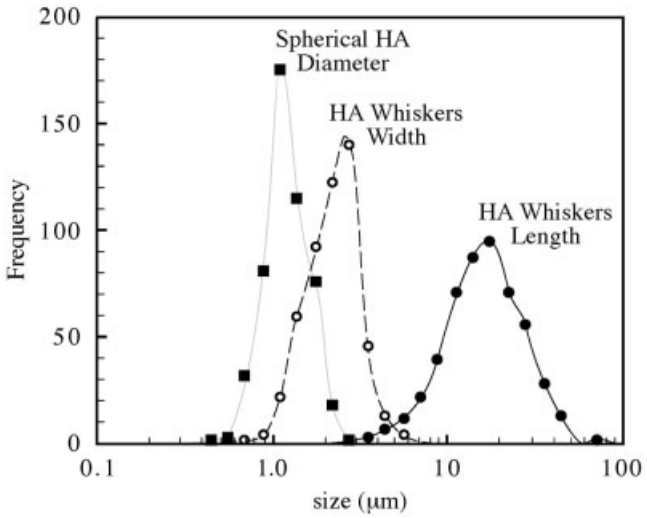

Figure 2. Particle size distributions measured for the as-prepared HA reinforcements, including the commercial, spherical HA powder, and the HA whiskers.

whisker composites prohibited machining and testing of tensile bars without premature failure in the mill or testing machine grips. Similarly, only one of the five possible tensile specimens was successfully machined and tested for 50 vol % spherical HA.

Composite mechanical properties

Exemplary stress–strain curves for the median specimen in each experimental group qualitatively depict the overall effects of the reinforcement type and volume fraction on the composite mechanical properties in tension (Fig. 4). Figure 5 and Table I show quantitative and statistical results for the elastic modulus (E), ultimate tensile stress (UTS), and work to failure (w_f) for varying volume fraction of both HA whisker and spherical HA reinforcements. Two-way ANOVA of all experimental groups except 0 vol % HA is shown in Table II. All measured mechanical properties showed statistically significant ($p < 0.05$) differences for the HA reinforcement type and volume fraction, separately. The elastic modulus and work to failure showed a statistically significant ($p < 0.05$) interaction between the reinforcement type and volume fraction. The ultimate tensile stress showed no such interaction.

As expected, increased reinforcement volume fraction resulted in an increase in elastic modulus for either type of reinforcement [Figs. 4 and 5(a)]. HA whiskers provided a greater than 10× increase in the

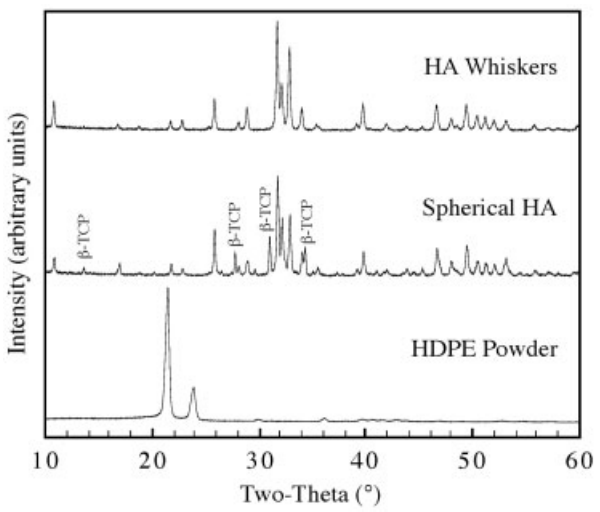

Figure 3. XRD patterns for the as-prepared starting powders, including the commercial, spherical HA, HA whiskers, and HDPE powders. All peaks for the HA powders correspond to phase-pure HA except those noted.

elastic modulus from ≈1 GPa in the polymer alone to greater than 10 GPa at 50 vol % HA. For greater than 10 vol % HA, HA whiskers resulted in a higher elastic modulus compared to the spherical HA ($p < 0.0001$) at any given volume fraction.

Increased reinforcement volume fraction resulted in an initial increase followed by a decrease in the ultimate tensile stress for either type of reinforcement [Figs. 4 and 5(b)]. A maximum ultimate tensile stress of approximately 30 and 25 MPa for HA whiskers and spherical HA, respectively, was achieved in the range of 20–30 vol % HA for either type of reinforcement. For greater than 10 vol % HA, HA whiskers resulted in a higher ultimate tensile stress compared to the spherical HA ($p < 0.05$) at any given volume fraction.

As also expected, increased reinforcement volume fraction resulted in a decrease in the work to failure for either type of reinforcement [Figs. 4 and 5(c)]. For greater than 10 vol % HA, HA whiskers resulted in a higher work to failure compared to the spherical HA ($p < 0.05$) at any given volume fraction except for the 40 vol % groups. The large changes in work to failure with reinforcement volume fraction, spanning three orders of magnitude in Figure 5(c), and changes in the shape of stress–strain curves in Figure 4 suggest that a transition from ductile to brittle failure occurred in the range of 30–40 vol % HA. In Figure 4, the transition appears to occur at a higher volume fraction for HA whiskers compared to spherical HA reinforcements, as shown by nonlinearity and postyield strain in the stress–strain curves, but has not been statistically verified in this study.

Table III compares the mechanical properties measured for the 20 vol % HA whisker-reinforced composites to those for composites that were annealed near the polymer melting temperature after processing. No significant differences were found for any of the mechanical properties measured ($p > 0.05$). Therefore, the polymer molecular structure, specifically the preferred molecular orientation, had little or no effect on the composite mechanical properties. The strengthening effects observed for HA whiskers over the spherical HA were thus concluded to be solely due to the morphology and preferred orientation of the reinforcement phase.

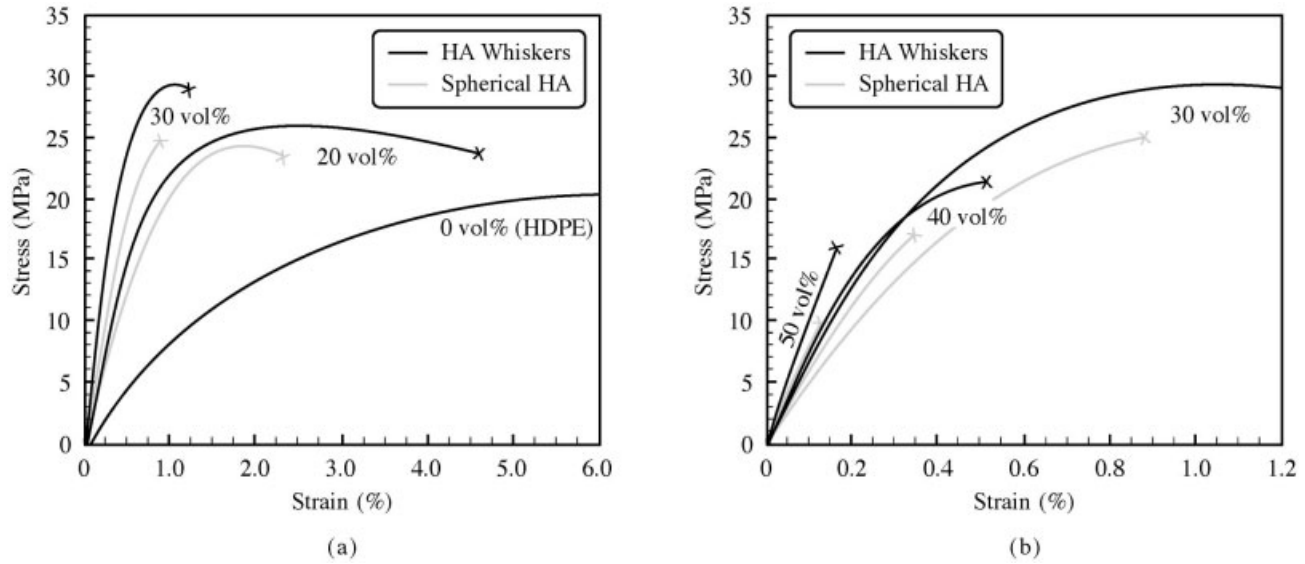

Figure 4. Exemplary stress–strain data for tensile tests of HA-reinforced HDPE using either HA whiskers or spherical HA reinforcements at (a) 0, 20, and 30 vol % and (b) 30, 40, and 50 vol %. Data is shown for the median specimen in each group.

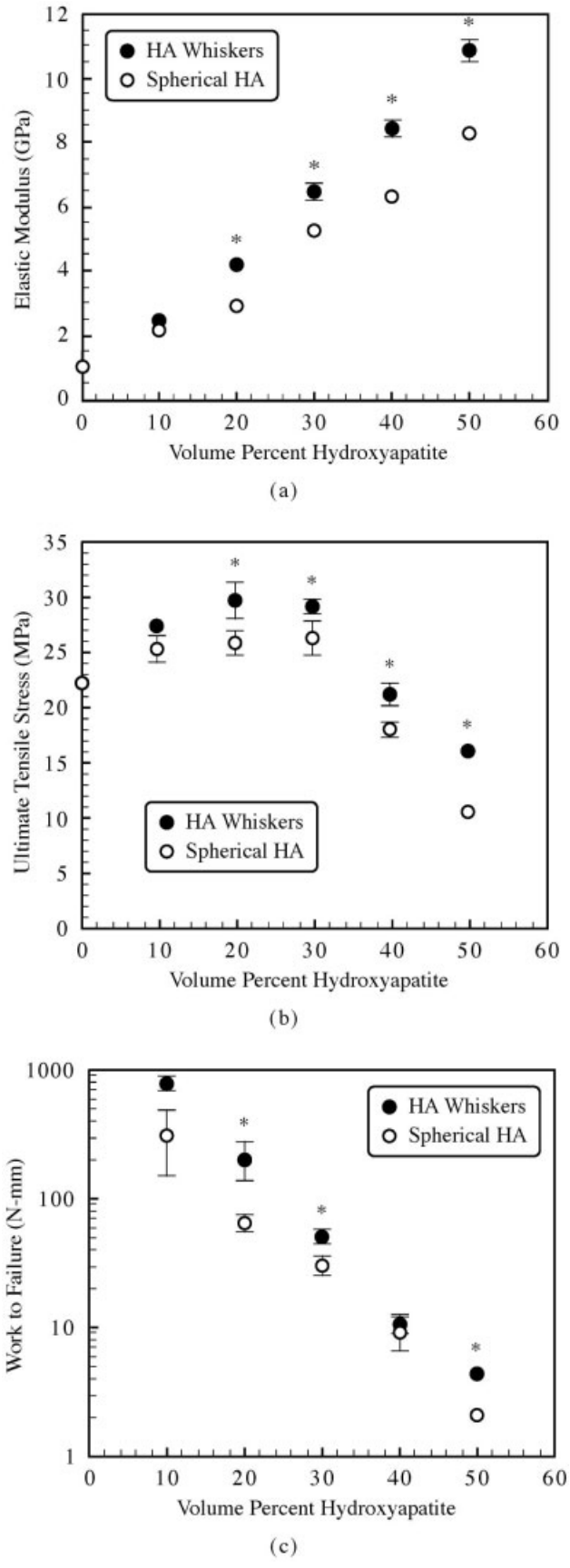

Figure 5. (a) Elastic modulus, (b) ultimate tensile strength, and (c) work to failure measured from tensile tests of HA-reinforced HDPE using either HA whiskers or spherical HA reinforcements at 0–50 vol %. Error bars span the first standard error. Asterisks denote a statistically significant difference ($p < 0.05$) between the HA whisker and spherical HA reinforcements at the same volume fraction.

Composite microstructure

Tensile test data suggested that the improved mechanical properties of the HA whisker-reinforced composites over spherical HA was due to mechanical anisotropy caused by the morphology and preferred orientation of the HA whisker reinforcements. A preferred orientation of HA whiskers in the HPDE matrix was verified by XRD on polished cross-sections of the three orthogonal specimen directions. Figure 6 shows XRD patterns for the three orthogonal specimen cross-sections compared to a randomly oriented powder of the HA reinforcements for a composite reinforced with 40 vol % HA whiskers and spherical HA. HA powder peaks were indexed[36] and are shown for the randomly oriented powder patterns in Figure 6. Note, however, overlap of peaks observed for HDPE relative to those for the HA reinforcements (Fig. 3). Previous studies have shown that the ⟨002⟩ crystallographic axis lies along the whisker length.[32] Therefore, the degree of preferred crystallographic orientation can be seen qualitatively by comparing the relative intensity of the {002} peak in the pattern, that is, the intensity of the {002} peaks relative to the most intense peak the same pattern. The HA whisker-reinforced composite [Fig. 6(a)] shows that {002} peaks had a much higher relative intensity on the longitudinal cross-sections (top pattern) compared to the relative intensity in the random powder (bottom pattern) and that {002} peaks had a lower relative intensity on the width and thickness cross-sections compared to the random powder. In contrast, XRD patterns for the spherical HA-reinforced composite [Fig. 6(b)] showed no discernable changes in the {002} relative intensity in the random powder and orthogonal specimen cross-sections. Thus, in HA whisker-reinforced HDPE HA whiskers were predominately aligned both crystallographically and morphologically along the length of the composite bar and tensile specimens. In spherical HA-reinforced HDPE, there was no observed preferred orientation of HA reinforcements, as expected.

Figure 7 shows XRD patterns for the three orthogonal specimen cross-sections compared to a randomly oriented powder of the bone mineral in a healthy human cortical bone specimen taken from the proximal end of the femoral midshaft. The {002} peaks had a much higher relative intensity on the longitudinal

TABLE I
Tensile Mechanical Properties for HA-Reinforced HDPE Composites Including the Elastic Modulus (*E*), Ultimate Tensile Stress (*UTS*), and Work to Failure (w_f)[a]

Reinforcement				
Vol %	Type	*E* (GPa)	*UTS* (MPa)	w_f (N-mm)
0	None	1.1 (0.1)	22.3 (0.1)	NA
10	HA whiskers	2.5 (0.1)	27.3 (0.5)	785.0 (105.5)
10	Spherical HA	2.2 (<0.1)	25.2 (1.1)	315.8 (168.7)
20	HA whiskers	4.2 (0.1)	29.6 (1.7)	202.9 (66.6)
20	Spherical HA	3.0 (0.1)	25.7 (1.1)	65.1 (9.9)
30	HA whiskers	6.5 (0.2)	29.1 (0.6)	50.1 (7.1)
30	Spherical HA	5.3 (0.1)	26.1 (1.6)	30.2 (4.8)
40	HA whiskers	8.4 (0.3)	21.0 (1.0)	10.7 (1.8)
40	Spherical HA	6.4 (0.2)	17.9 (0.6)	9.0 (2.7)
50	HA whiskers	10.8 (0.4)	16.2 (0.3)	4.2 (0.3)
50	Spherical HA	8.3	10.5	2.1

[a]Reported values include the group mean with the standard error given in parentheses. NA, not applicable.

cross-section (top pattern) compared to the relative intensity in the random powder (bottom pattern) and a lower relative intensity on the width and thickness cross-sections compared to the random powder. The relative peak intensities of the human bone mineral were observed to be similar to those for the HA whisker-reinforced composites. Therefore, the preferred orientation in HA whisker-reinforced composites [Fig. 6(a)] appears similar to that found in human bone tissue (Fig. 7).

The qualitative effects of the morphology and preferred orientation of the HA whiskers on the mechanical properties were also evident in the failure surfaces of tensile specimens. SEM revealed dramatic changes in the failure surface topography with increasing reinforcement volume fraction and with the different reinforcement types. The failure surfaces for composites reinforced with 20 and 50 vol % HA demonstrate the basic trends and are shown in Figure 8. HDPE fibrils protruded from all failure surfaces. The size (length and diameter) of the fibrils decreased dramatically with increasing HA volume fraction for either reinforcement type. The most sizeable differences were observed at less than 30 vol % HA (not shown). The length of HDPE fibrils was observed to be longer in composites reinforced with HA whiskers relative to spherical HA. In HA whisker-reinforced composites, HA whiskers were observed to protrude from the failure surfaces, as shown in Figure 9.

TABLE II
Statistical Results of Two-Way ANOVA for the Elastic Modulus (*E*), Ultimate Tensile Stress (*UTS*), and Work to Failure (w_f) Grouping for the Reinforcement Type and Volume Fraction

Grouping	*E*	*UTS*	w_f
HA reinforcement type	$p < 0.0001$	$p = 0.0002$	$p = 0.0117$
HA volume fraction	$p < 0.0001$	$p < 0.0001$	$p < 0.0001$
HA type · volume fraction	$p < 0.0001$	$p = 0.8183$	$p = 0.0109$

DISCUSSION

HDPE reinforced with HA whiskers had higher elastic modulus (*E*), ultimate tensile strength (*UTS*), and work to failure (w_f) relative to composites reinforced with spherical HA (Figs. 4 and 5). As expected, increased volume fraction of either reinforcement type over 0–50 vol % resulted in increased elastic modulus, a maximum in ultimate tensile stress, and decreased work to failure (Figs. 4 and 5). Thus, HA whisker-reinforced HDPE composites possessed improved mechanical properties over those reinforced with spherical HA. In particular, the enhanced elastic modulus and work to failure associated with HA whisker reinforcement resulted in mechanical behavior more like that of bone tissue than the spherical reinforcements.

The elastic modulus of composites containing 30–50 vol % HA whiskers was in the range of 6–11 GPa [Fig.

TABLE III
Tensile Mechanical Properties, Including the Elastic Modulus (*E*), Ultimate Tensile Stress (*UTS*), and Work to Failure (w_f), for HDPE Reinforced with 20 vol % HA whiskers, Showing the Effects of Annealing After Processing[a]

Group	*E* (GPa)	*UTS* (MPa)	w_f (N-mm)
As processed	4.2 (0.1)	29.6 (1.7)	203 (67)
Annealed	4.3 (0.4)	26.5 (0.6)	86 (15)
p value	$p > 0.05$	$p > 0.05$	$p > 0.05$

[a]Reported values include the group mean with the standard error given in parentheses.

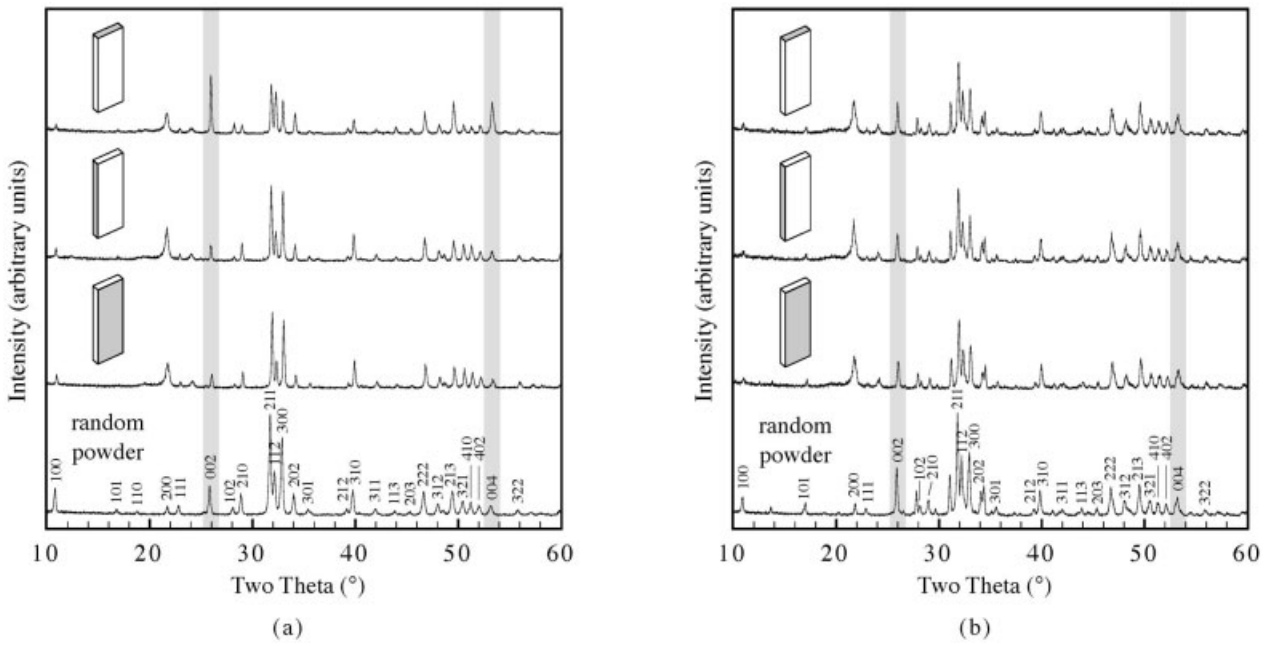

Figure 6. XRD patterns for composites reinforced with 40 vol % (a) HA whiskers and (b) spherical HA, showing the degree of preferred crystallographic orientation of the HA reinforcements. The specimen cross-section is shown schematically on the left of each pattern and {002} peaks are highlighted.

5(a)], which corresponds to the range of values for human cortical bone. Recall that the longitudinal and transverse elastic moduli for human cortical bone are 17–27 and 6–13 GPa, respectively.[1,6,7] The longitudinal elastic modulus of the composites of this study reached values for the transverse modulus of cortical bone. Thus, significant improvements are still needed. Nonetheless, this work comprises a significant step forward for particulate-reinforced polymers processed by conventional techniques. Further improvements are expected to be achieved by tailoring the whisker morphology and preferred orientation and using other polymer matrices.

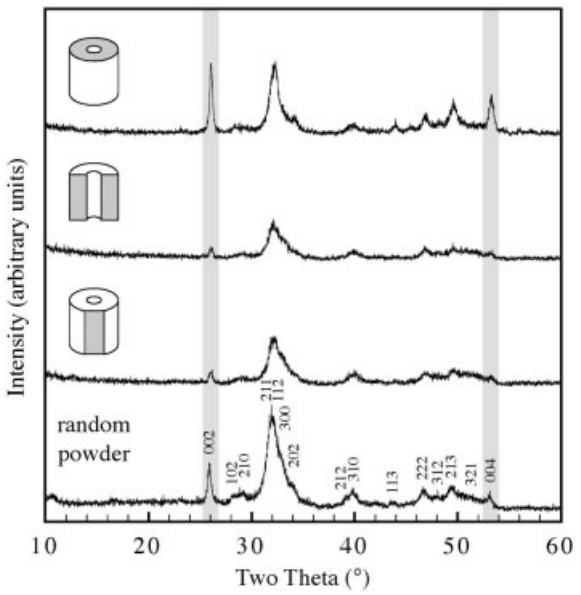

Figure 7. XRD patterns for a human cortical bone specimen taken from the proximal end of the femoral midshaft, showing the degree of preferred crystallographic orientation of the bone mineral. The specimen cross-section is shown schematically on the left of each pattern and {002} peaks are highlighted.

The stress–strain data for composites containing 30 vol % HA whiskers (Fig. 4), for example, looked like that for bone tissue, including nonlinearity and a strain to failure greater than 1%. Note, however, that bone achieves this behavior at approximately 50 vol % reinforcement.[7] This difference shows the effect of chemical coupling that exists between collagen and bone mineral, whereas the composites produced in this study possessed only mechanical coupling between the HDPE and HA, as was also noted in previous works.[13,14]

The mechanical anisotropy of the HA whisker-reinforced composites was the result of a preferred crystallographic and morphological orientation of the whiskers in the polymer matrix (Fig. 6). HA whiskers were predominately aligned along the direction of flow during molding of the polymer matrix. This preferred orientation was qualitatively observed to be similar to that found in human cortical bone. The preferred orientation of bone mineral is known to result from physiological stimuli that originate with mechanical loading.[37–39] In the HA whisker-reinforced

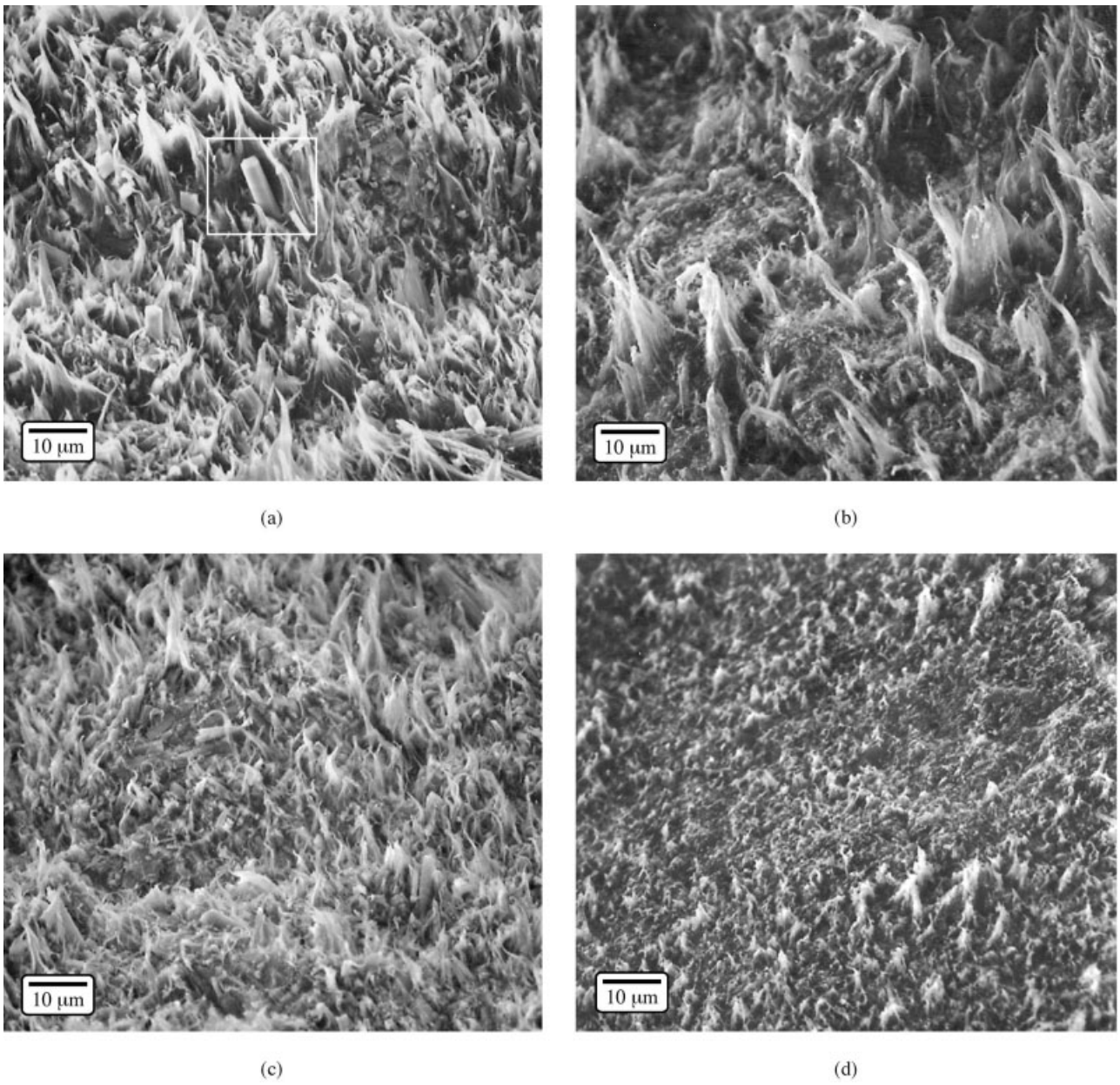

Figure 8. SEM micrographs showing the failure surface of composites reinforced with (a) 20 vol % HA whiskers, (b) 20 vol % spherical HA, (c) 50 vol % HA whiskers, and (d) 50 vol % spherical HA. The boxed area in (a) is shown at higher magnification in Fig. 9.

composites, whisker alignment was induced during processing by shear stresses acting along the flow field as the material extruded in the forge mold. In a subsequent article we will report the stiffness coefficients of HA whisker-reinforced composites and correlate these to quantitative measurements of the preferred orientation.

This work also facilitates a unique means to study the structure and function of bone tissue. Several fundamental questions may be addressed through biomimetic materials such as HA whisker-reinforced composites. What is the relationship between the bone mineral content, morphology and preferred orientation, and the tissue properties? What is the minimum hierarchical scale at which overall material properties similar to those measured for cortical bone can be obtained? What are the role and effects of the interface between collagen and bone mineral on the overall mechanical properties?

A novel processing technique for particulate composites was also demonstrated in this study. In contrast to previous works, the reinforcement phase and

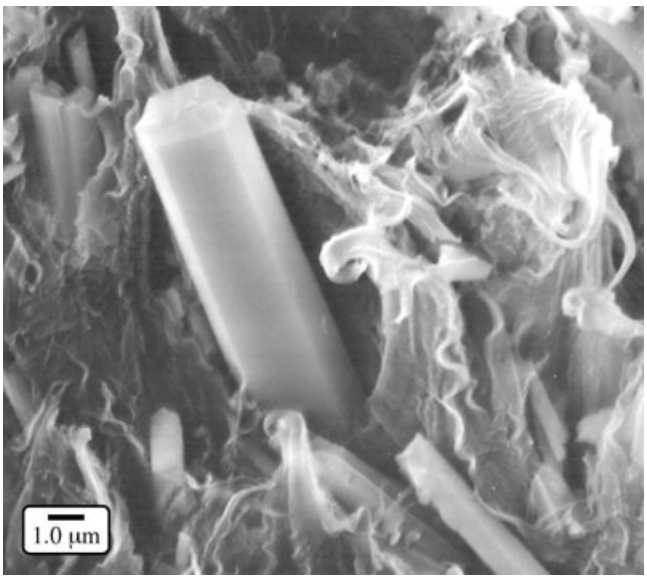

Figure 9. Higher-magnification SEM micrograph of Fig. 8(a), showing whisker pullout on the failure surface for a composite reinforced with 20 vol % HA whiskers.

matrix were co-dispersed and co-consolidated in powder form prior to the compression molding step. This approach is believed to have resulted in improved dispersion of reinforcement phase within the matrix relative to more traditional techniques such as compounding,[11–14] especially at high reinforcement volume fractions. Indeed, higher-volume fractions of HA were able to be processed in this study relative to previous works for HA-reinforced polyethylene.[11–14] Further, while other factors cannot be ruled out, the elastic modulus for the spherical HA-reinforced composites of this study was measured to be greater than that reported for composites in previous works at the same HA volume fraction.

In summary, synthetic HA whiskers have been utilized as a new, biocompatible reinforcement for orthopedic biomaterials. The use of HA whiskers to engineer new biomaterials with a preferred orientation of reinforcements and tailored mechanical anisotropy is hoped to provide more than a biomimetic novelty. Through control of the size, aspect ratio, volume fraction, and preferred orientation of the HA whiskers within a matrix material, anisotropic and enhanced mechanical properties can be achieved and tailored to the implant site. The stiffness anisotropy in HA whisker-reinforced composites could enable matching of the anisotropy present in human cortical bone, thereby eliminating or greatly decreasing the problem of stress shielding for synthetic orthopedic implant materials. Consequently, a variety of matrix materials for a range of potential applications are being explored.

References

1. Yaszemski MJ, Payne RG, Hayes WC, Langer R, Mikos AG. Evolution of bone transplantation: molecular, cellular and tissue strategies to engineer human bone. Biomaterials 1996;17: 175–185.
2. Rose FRAJ, Oreffo ROC. Bone tissue engineering: Hope vs. hype. Biochem Biophys Res Commun 2002;292:1–7.
3. Perry CR. Bone repair techniques, bone graft, and bone graft substitutes. Clin Orthoped 1999;360:71–86.
4. Huiskes R, Weinans H, Dalstra M. Adaptive bone remodeling and biomechanical design considerations for noncemented total hip arthroplasty. Orthopedics 1989;12:1255–1267.
5. Huiskes R. Bone remodeling around implants can be explained as an effect of mechanical adaptation. In: Galante JO, Rosenberg AG, Callahan JJ, editors. Total hip revision surgery. New York: Raven Press; 1995. Chapter 15.
6. Guo XE. Mechanical properties of cortical bone and cancellous bone tissue. In: Cowin SC, editor. Bone mechanics handbook. 2nd ed. Boca Raton, FL: CRC Press; 2001. p 11–23.
7. Rho J-Y, Kuhn-Spearing L, Zioupos P. Mechanical properties and the hierarchical structure of bone. Med Eng Phys 1998;20: 92–102.
8. Turner CH, Rho J, Takano Y, Tsui TY, Pharr GM. The elastic properties of trabecular and cortical bone tissues are similar: Results from two microscopic measurement techniques. J Biomech 1999;32:437–441.
9. Agrawal CM, Ray RB. Biodegradable polymeric scaffolds for musculoskeletal tissue engineering. J Biomed Mater Res 2001; 55:141–150.
10. Evans SL, Gregson PJ. Composite technology in load-bearing orthopedic implants. Biomaterials 1998;19:1329–1342.
11. Bonfield W, Grynpas MD, Tully AE, Bowman J, Abram J. Hydroxyapatite reinforced polyethylene—a mechanically compatible implant material for bone replacement. Biomaterials 1981;2:185–186.
12. Bonfield W, Bowman JA, Grynpas MD. Composite material for use in orthopedics. U.S. patent 5,017,627. 1991.
13. Wang M, Porter D, Bonfield W. Processing, characterisation, and evaluation of hydroxyapatite reinforced polyethylene composites. Br Ceram Trans 1994;93(3):91–95.
14. Wang M, Joseph R, Bonfield W. Hydroxyapatite–polyethylene composites for bone substitution: Effects of ceramic particle size and morphology. Biomaterials 1998;19:2357–2366.
15. Kikuchi M, Suetsugu Y, Tanaka J, Akao M. Preparation and mechanical properties of calcium phosphate/copoly-L-lactide composites. J Mater Sci Mater Med 1997;8:361–364.
16. Shikinami Y, Okuno M. Bioresorbable devices made of forged composites of hydroxyapatite (HA) particles and poly-L-lactide (PLLA): Part I. Basic characteristics. Biomaterials 1999;20: 859–877.
17. Ignjatovic N, Tomic S, Dakic M, Miljkovic M, Plavsic M, Uskokovic D. Synthesis and properties of hydroxyapatite/poly-L-lactide composite biomaterials. Biomaterials 1999;20:809–816.
18. Durucan C, Brown PW. Calcium-deficient hydroxyapatite–PLGA composites: Mechanical properties and microstructural characterization. J Biomed Mater Res 2000;51:726–734.
19. Saito M, Maruoka A, Mori T, Sugano N, Hino K, Oonishi H. Hydroxyapatite composite resin as a new bioactive bone cement. In: Ducheyne P, Christiansen D, editors. Bioceramics. vol. 6. Proceedings of the 6th International Symposium on Ceramics in Medicine. Oxford, UK: Butterworth-Heinemann Ltd.; 1993. p 475–480.
20. Harper EJ, Behiri JC, Bonfield W. Flexural and fatigue properties of a bone cement based upon polyethylmethacrylate and hydroxyapatite. J Mater Sci Mater Med 1995;6:799–803.

21. Kobayashi M, Nakamura T, Okada Y, Fukumoto A, Furukawa T, Kato H, Kokobu T, Kikutani T. Bioactive bone cement: Comparison of apatite and wollastonite containing glass-ceramic, hydroxyapatite, and β-tricalcium phosphate fillers on bone bonding strength. J Biomed Mater Res 1998;42:223–237.
22. Shinzato S, Kobayashi M, Mousa WF, Kamimura M, Neo M, Kitamura Y, Kokubo T, Nakamura T. Bioactive polymethyl methacrylate-based bone cement: Comparison of glass beads, apatite- and wollastonite-containing glass-ceramic, and hydroxyapatite fillers on mechanical and biological properties. J Biomed Mater Res 2000;51:258–272.
23. Ascenzi A, Bonucci E, Generali P, Ripamonti A, Roveri N. Orientation of apatite in single osteon samples as studied by pole figures. Calcif Tissue Int 1979;29:101–105.
24. Sasaki N, Matsushima N, Ikawa T, Yamamura H, Fukuda A. Orientation of bone mineral and its role in the anisotropic mechanical properties of bone—transverse anisotropy. J Biomech 1989;22:157–164.
25. Sasaki N, Sudoh Y. X-ray pole figure analysis of apatite crystals and collagen molecules in bone. Calcif Tissue Int 1997;60:361–367.
26. Takano Y, Turner CH, Burr DB. Mineral anisotropy in mineralized tissues is similar among species and mineral growth occurs independently of collagen orientation in rats: Results from acoustic velocity measurements. J Bone Miner Res 1996; 11:1292–1301.
27. Ashman RB, Cowin SC, Van Buskirk WC, Rice JC. A continuous wave technique for the measurement of the elastic properties of cortical bone. J Biomech 1984;17:349–361.
28. Van Buskirk WC, Cowin SC, Ward RN. Ultrasonic measurement of orthotropic elastic constants of bovine femoral bone. J Biomech Eng 1981;103(5):67–72.
29. Dornhoffer JL. Hearing results with the Dornhoffer ossicular replacement prostheses. Laryngoscope 1998;108, pt. 1(4):531–536.
30. Fujishiro Y, Yabuki H, Kawamura K, Sato T, Okuwaki A. Preparation of needle-like hydroxyapatite by homogeneous precipitation under hydrothermal conditions. J Chem Tech Biotech 1993;57:349–353.
31. Yoshimura M, Ioku K, Okamoto K, Takeuchi H. Apatite whisker and method for preparation thereof. U.S. patent 5,227,147. 1993.
32. Yoshimura M, Suda H, Okamoto K, Ioku K. Hydrothermal synthesis of biocompatible whiskers. J Mater Sci 1994;29:3399–3402.
33. Suchanek W, Sada H, Yashimi M, Kakihana M, Yoshimura M. Biocompatible whiskers with controlled morphology and stoichiometry. J Mater Res 1995;10:521–529.
34. Kandori K, Horigami N, Yasukawa A, Ishikawa T. Texture and formation mechanism of fibrous calcium hydroxyapatite particles prepared by decomposition of calcium–EDTA chelates. J Am Ceram Soc 1997;80:1157–1164.
35. LeGeros RZ, LeGeros JP. Dense hydroxyapatite. In: Hench LL, Wilson J, editors. Advanced series in ceramics. vol. 1.An introduction to bioceramics. River Edge, NJ: World Scientific; 1993. p 139–180.
36. Powder diffraction file 09-0432. Newton Square, PA: JCPDS-International Centre for Diffraction Data (ICDD); 1997.
37. Wolff J. The law of bone remodeling. New York: Springer–Verlag; 1986.
38. Duncan RL, Turner CH. Mechanotransduction and the functional response of bone to mechanical strain. Calcif Tissue Int 1995;57:344–358.
39. van der Meulen MCH, Huiskes R. Why mechanobiology? A survey article. J Biomech 2002;35:401–414.